



CrossMark
click for updates

Cite this: *J. Mater. Chem. A*, 2015, 3, 1427

Received 2nd October 2014
Accepted 25th November 2014

DOI: 10.1039/c4ta05244g

www.rsc.org/MaterialsA

Preparation of a porous nanostructured germanium from GeO₂ via a “reduction–alloying–dealloying” approach†

Huayi Yin, Wei Xiao,* Xuhui Mao, Hua Zhu and Dihua Wang*

We present here a controllable and affordable preparation of porous nanostructured germaniums with interesting photo-responsive properties from GeO₂ powder through an electrochemical reduction–alloying process in molten salt (reduction and alloying) and post zero-energy-consumption water etching (dealloying).

Over the past few decades, the preparation and utilization of porous nanostructured germanium has attracted an enormous amount of attention due to its unique physicochemical properties and promising applications in electronic, optical, electrochemical and biological devices.^{1–5} Several approaches have been proposed for preparing nanoporous germanium such as electrochemical etching of Ge wafers,^{6–8} chemical vapor deposition,^{4,9,10} chemical reduction of porous GeO₂,¹¹ liquid-crystal-templated chemical method^{3,4} and electrochemical deposition in room temperature ionic liquids.¹² The widespread application of porous nanostructured germanium remains a challenge hitherto to some extent due to the unsatisfactory economic competence (low space-time yield, intense investment in apparatus and labor, expensive feedstock and tedious procedures) and inferior environmental viability (toxic precursors and by-products) of the forenamed methods. Therefore, a cost-effective, environmentally friendly and upscalable production of porous nanostructured germanium is of significant urgency and importance, aiming to fully exploit its intriguing functionalities.

Recently, a generic approach for the preparation of nanoporous materials using an initial electrochemical lithiation of a matrix followed by an electrochemical delithiation of the Li-rich matrix was proposed and confirmed.¹³ The reversibility in volume change with the maintenance in the integrity of a matrix during the electrochemical lithiation–delithiation process

forms the scientific basis for the generation of high-quality nanoporous materials. However, the extension of the aforementioned strategy for the preparation of nanoporous metals/semimetals in group IV (*e.g.* Si, Ge and Sn) is highly challenging due to the occurrence of inevitable vast changes (higher than 300%) in the volume of the abovementioned matrix upon electrochemical polarization with cations (*e.g.* Li⁺), which are electrochemically introduced/removed into/from the matrix (Si, Ge and Sn) *via* alloying/dealloying reactions.^{14–16} This results in the destruction of the matrix architecture (so-called “pulverization”), and it further results in the inferior cycle performance of such materials when used in Li and Na ion batteries.

Such a pulverization effect creates an intrinsic barrier for the preparation of porous Ge *via* the abovementioned electrochemical lithiation–delithiation strategy; however, it might be tackled using an etching strategy instead of electrochemical delithiation as the post step for the removal of the previously alloyed components. The effectiveness of the etching strategy has been well demonstrated in the successful preparation of porous germanium by chemically etching germanium alloys (Ge₄K₉) through ion exchange and thermal decomposition reactions.³ The ion-exchange and thermal-decomposition etching process of Ge₄K₉ involved in the preparation of porous Ge can be further improved into a fascinating “zero-energy-consumption” etching method using Ca–Ge as the precursor. In such a scenario, alloyed Ca can be chemically removed by reaction with water, creating voids in the Ge and generating a porous Ge. This “zero-energy-consumption” etching strategy resembles the method used in producing RANEY® nickel by selectively dissolving Al from NiAl intermetallic compound in an alkaline solution through effective and generic chemical dealloying routes.^{17,18}

Herein, for the first time, we propose a cost-effective and environmentally friendly strategy for producing a porous nanostructured Ge from solid GeO₂ *via* a “reduction–alloying–dealloying” method. As schematically represented in Fig. 1, the first two steps occurring in molten CaCl₂–NaCl eutectics at 600 °C involve the electrochemical reduction of solid GeO₂ into

School of Resource and Environmental Sciences, Wuhan University, Wuhan 430072, PR China. E-mail: wangdh@whu.edu.cn; gabrielxiao@whu.edu.cn; Fax: +86 27 68774216; Tel: +86 27 68775799

† Electronic supplementary information (ESI) available: Experimental details and more characterizations. See DOI: 10.1039/c4ta05244g

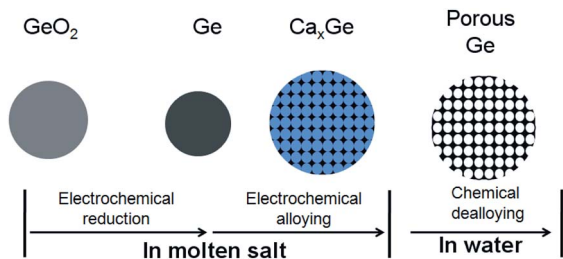


Fig. 1 Schematic illustration of the process for the formation of porous Ge.

nanostructured Ge (Step I: “reduction”) and *in situ* electrochemically intercalation (alloying) of cations from the melts into Ca–Ge alloys (Step II: “alloying”) at more negative potentials. The abovementioned “reduction” and “alloying” occur in the molten salts in the presence of cathodic polarizations, which occur in series and/or in parallel. The electrolytic Ca–Ge is then subjected to a “zero-energy-consumption” etching in water at room temperature (Step III: “dealloying”), with the maintenance of the matrix and generation of nanoporous Ge after the removal of Ca species.

The merits of the proposed strategy for the production of nanoporous Ge can be justified as follows: First, as an analogue of widely used silicon, Ge has a higher dielectric constant, lower resistivity, higher electron/hole mobility and intriguing energy storage capabilities with promising applications of Ge in electronic, optoelectronic and energy fields. However, its practical applications have been drastically hindered by the costly and high-risk extraction process based on the chemical reduction of GeO_2 with hydrogen at 600–700 °C.¹⁹ Second, GeO_2 powder is the most straightforward and favorite feedstock for Ge extraction due to its low cost and low toxicity. Third, the relatively high temperature in the molten salt electrolyzer enhances the kinetics of the electrochemical alloying process (note the inevitably sluggish kinetics of the solid diffusion process during alloying), facilitating the rapid preparation of massive Ca–Ge compound, and therefore promising a high space-time yield. In addition, the exothermic nature of the alloying process not only further enhances the reaction kinetics, but it also helps to maintain the high temperature of the melt. Fourth, “electrons” are employed as the green (considering the increasing installed capacity from renewable energy in grids) and no-trace (introducing no impurity) reductant here. More importantly, the activity of electrons can be easily tuned by just tailoring the electrode potentials, promising a controllable preparation of Ca–Ge (note that Ca and Ge can form binary solutions in any stoichiometry) in different stoichiometries, and therefore generation of Ge with different porosity. Last but not the least, the molten salt electrolysis of solid oxides (e.g. silica or GeO_2) is well addressed as an upscalable and controllable preparation method for nanostructured (nanoparticles and nanowires) semiconductor (Si and Ge) powders.^{20–29} Therefore, the proposed method is upscalable and controllable. The molten salt electrolysis of solid oxides is well addressed to be an effective and environmentally friendly method for the

preparation of metals and alloys in the recent years.^{22,26–29} However, the preparation of nanoporous materials from the molten salt electrolysis of solid oxides is absent in the literature, which is for the first time reported here with the combination of the molten salt electrolysis of solid oxides and a facile etching process in water. Thus, this method is new and it might have significant impacts on the preparation of porous materials.

Experimental details are provided in the ESI.† The electrochemical behavior of solid GeO_2 was studied by cyclic voltammetry (CV) using a Mo cavity electrode filled with GeO_2 powder (Fig. S1†). As can be seen in Fig. 2, the first reduction peak starting at -0.9 V vs. Ag/AgCl (c1) was associated with the reduction of GeO_2 to Ge.²¹ Subsequently, three additional redox peak pairs consecutively appear at potentials more negative than that during the generation of Ge, followed by a redox peak pair assigned to the electrodeposition/re-dissolution of liquid metals from metals near the negative limits. The onsets of the three consecutive cathodic processes after Ge generation are -1.6 , -1.8 and -2.0 V, corresponding to the three separate alloying processes. Such a scenario agrees well with the phase diagrams of Ge–Ca and Ge–Na, which indicates more than three alloys of Ge–Ca and Ge–Na.^{30,31} Upon the inverse anodic scan, three consecutive oxidation peaks correspond to three dealloying processes. The similar shape and integral charges reveal that the alloying/dealloying reactions are highly reversible. The abovementioned results suggest that the concentration of Ca or Na in Ge can be controlled by adjusting the electrolysis potentials, promising the engineering of the microstructure and porosity in the final products.

To specify the stoichiometries of the electrolytic samples, the potentiostatic electrolysis of the GeO_2 filled Mo cavity electrodes was performed. Four electrodes were potentiostatically electrolyzed at -1.35 , -1.7 , -1.9 and -2.1 V for 15 min. Because the products are stable in dimethyl sulfoxide (DMSO), which is able to dissolve residual salts, the obtained products were washed with DMSO instead of aqueous solutions and analyzed using

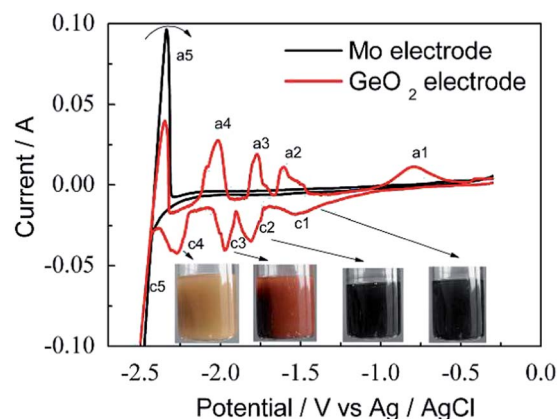


Fig. 2 CVs of the Mo and GeO_2 modified Mo cavity electrodes in a CaCl_2 – NaCl melt at 600 °C at a scan rate of 20 mV s^{-1} . The insets are the digital images of the products (obtained at -1.35 , -1.7 , -1.9 and -2.1 V) dispersed in water.

EDX (Fig. S2†) and XRD (Fig. S3†). Clearly, the product obtained at -1.35 V is pure Ge. However, Ca is observed in the products obtained at potentials more negative than -1.6 V. Na remains absent in all the samples, indicating that Ca is the only alloying element in the electrochemical reduction process over the investigated potential range. CaO was found in the products obtained at -1.9 and -2.1 V after treating with DMSO, further indicating that the Ca was alloyed into Ge, and the alloyed Ca can be oxidized in air (Fig. S3†).

Interestingly, the aqueous suspensions of the above electrolytic products show different colors (insets of Fig. 1). It should be noted that all of the electrolytic products are grayish black without rinsing with water, indicating that rinsing with water leads to the color change. The aqueous suspensions of the electrolytic product obtained at -1.35 and -1.7 V remain grayish black. It is observed that the product obtained at -1.35 V does not react with water. In addition, a slight reaction between water and the product obtained at -1.7 V can be observed, whereas the color of the products obtained at -1.9 and 2.1 V change to red and yellow, respectively. Moreover, the products obtained at -1.9 and -2.1 V rigorously react with water along with violent gas evolution, which can be expressed by eqn (1):



According to the corresponding XRD patterns (Fig. S4†), the products obtained at -1.35 and -1.7 V are crystalline Ge, whereas the red and yellow products are less crystalline with the occurrence of two weak and broaden diffraction peaks. The thermodynamically spontaneous nature of reaction (1) forms the scientific grounds of the effective separation of Ge and Ca species, which also facilitates the formation of porous Ge after rinsing in water. In addition, the gas evolution was also beneficial for the formation of pores. This process is considerably similar to the process of producing porous Ni by etching Al from NiAl.¹⁸

After the products were washed with water, all the products were found to be pure Ge (Fig. S5†), which further confirms that the alloyed Ca can be removed by water etching. The SEM images of the products show that the products obtained at -1.35 and -1.7 V were Ge nanowires (Fig. 3a and b), whereas the products obtained at potentials of -1.9 and -2.1 V tend to agglomerate and appear like coral and floccules, respectively (Fig. 3c and d). A trace amount of Ca and Cl was observed due to trace residual salt (Fig. S5c and S5d†). To further investigate the effect of electrolysis potential on the morphology of the products, the products were characterized by TEM and HRTEM (Fig. 3). The diameter of the Ge nanowires obtained at -1.35 V is around 100 nm (Fig. 3a), and the product obtained at -1.7 V are interconnected and no single nanowire can be observed (Fig. 3b), suggesting the inclusion of Ca affects the growth of Ge. At -1.9 V, the product turns into prism-like particles (Fig. 3c), and at -2.1 V, the product appears like cotton (Fig. 3d). As can be seen from the HRTEM shown in Fig. 3e and f, the products obtained at -1.9 and -2.1 V are in the form of porous structures. The decrease in crystallinity after rinsing with water was also verified by HRTEM (Fig. S6†). Therefore, a porous Ge was

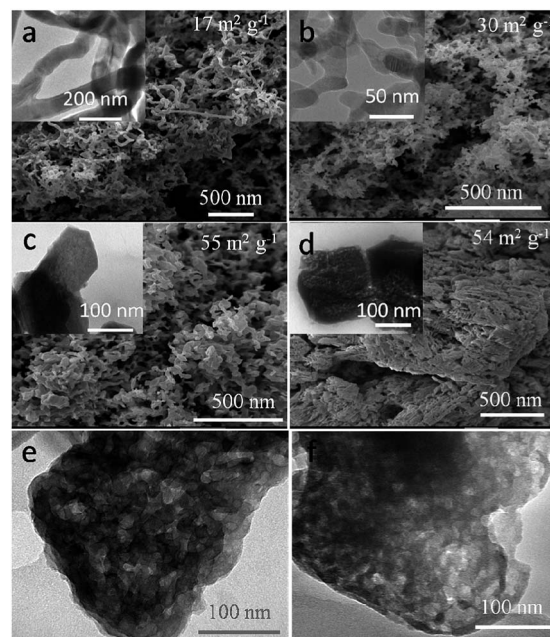


Fig. 3 SEM images of the Ge obtained at -1.35 V (a), -1.7 V (b), -1.9 V (c) and -2.1 V (d). The insets are their corresponding TEM images. The HRTEM images of the Ge obtained at -1.9 V (e) and -2.1 V (f).

successfully prepared by the electrolysis of GeO_2 particles (Fig. S7†) at -1.9 V and -2.1 V followed by a water etching pathway. The BET surface area of the corresponding products presented in Fig. 3 indicates that the porous Ge has considerably larger surface area ($\sim 55 \text{ m}^2 \text{ g}^{-1}$) than Ge nanowires ($17 \text{ m}^2 \text{ g}^{-1}$). Moreover, the BET surface area of the product obtained at -1.7 V ($30 \text{ m}^2 \text{ g}^{-1}$) is larger than the product obtained at -1.35 V, which is also associated with the dealloying of Ca from Ge. CO_2 emission on the graphite anode is acknowledged. The development of inert anodes to achieve zero carbon footprints deserves further research. However, the electrochemical method has the great advantage of adjusting the current density and/or potential to tailor the electrolytic products.

The samples obtained were further investigated by Raman (Fig. S8a and S8b†) and FT-IR (Fig. S8c and S8d†) spectroscopy. All the spectra confirm the formation of Ge. Some minor difference exists in the spectra between porous Ge (obtained at -1.90 and -2.1 V) and crystalline Ge (obtained at -1.35 and -1.7 V), indicating that the optical properties can be tuned by changing the preparation parameters. Such differences in the optical properties can also be reflected by the different colors of the samples (Fig. 1), promising the application of the obtained samples in photoluminescence and photocatalysis. It is acknowledged that the research on optical properties is preliminary. The relationship between the structure and optical properties needs further investigation in future.

Conclusions

In summary, we provide the first proof-of-concept of the controllable and affordable preparation of porous

nanostructured germanium, with interesting photo-responsive properties from GeO_2 powder through an electrochemical reduction-cum-alloying process in molten salt and post zero-energy-consumption water etching. First, solid GeO_2 powder is electrochemically deoxygenated to Ge in CaCl_2 -NaCl eutectics at 600 °C; simultaneously, Ca^{2+} is electrochemically alloyed/intercalated into the pre-reduced Ge at a more negative potential. The obtained Ca_xGe is then dealloyed in an aqueous solution generating porous germanium without the destruction of the original matrix integrity. The confirmed tunable nature of electrochemical alloying/dealloying between the Ca and Ge species not only facilitates the preparation of nanostructured Ge with different pore characteristics, but also provides unprecedented opportunities to tune the optical properties of nanoporous Ge. In addition, the high reversibility of the observed electrochemical alloying/dealloying of Ca into Ge promises the development of Ca ion rechargeable batteries in future.

Acknowledgements

The financial support from the NSFC (51071112, 21203141 and 51325102), MOST (2009DFA62190) and Wuhan University (121075) are acknowledged.

Notes and references

- 1 S. Miyazaki, K. Sakamoto, K. Shiba and M. Hirose, *Thin Solid Films*, 1995, **255**, 99–102.
- 2 S. S. Chang and R. E. Hummel, *J. Lumin.*, 2000, **86**, 33–38.
- 3 G. S. Armatas and M. G. Kanatzidis, *Science*, 2006, **313**, 817–820.
- 4 G. S. Armatas and M. G. Kanatzidis, *Adv. Mater.*, 2008, **20**, 546–550.
- 5 G. S. Armatas and M. G. Kanatzidis, *Nat. Mater.*, 2009, **8**, 217–222.
- 6 C. Fang, H. Föll and J. Carstensen, *J. Electroanal. Chem.*, 2006, **589**, 259–288.
- 7 C. Fang, H. Foll, J. Carstensen and S. Langa, *Phys. Status Solidi A*, 2007, **204**, 1292–1296.
- 8 H. C. Choi and J. M. Buriak, *Chem. Commun.*, 2000, 1669–1670.
- 9 J. Shieh, H. L. Chen, T. S. Ko, H. C. Cheng and T. C. Chu, *Adv. Mater.*, 2004, **16**, 1121–1124.
- 10 M. E. Davis, *Nature*, 2002, **417**, 813–821.
- 11 C. B. Jing, C. J. Zhang, X. D. Zang, W. Z. Zhou, W. Bai, T. Lin and J. H. Chu, *Sci. Technol. Adv. Mater.*, 2009, **10**, 065001.
- 12 F. Endres and S. Z. El Abedin, *Phys. Chem. Chem. Phys.*, 2002, **4**, 1640–1648.
- 13 (a) Y.-S. Hu, Y.-G. Guo, W. Sigle, S. Hore, P. Balaya and J. Maier, *Nat. Mater.*, 2006, **5**, 713–717; (b) H. Xia, M. O. Lai and L. Lu, *J. Power Sources*, 2011, **196**, 2398–2402.
- 14 J. W. Choi, J. McDonough, S. Jeong, J. S. Yoo, C. K. Chan and Y. Cui, *Nano Lett.*, 2010, **10**, 1409–1413.
- 15 X. H. Liu, S. Huang, S. T. Picraux, J. Li, T. Zhu and J. Y. Huang, *Nano Lett.*, 2011, **11**, 3991–3997.
- 16 Q. Chen and K. Sieradzki, *Nat. Mater.*, 2013, **12**, 1102–1106.
- 17 A. A. Pavlic and H. Adkins, *J. Am. Chem. Soc.*, 1946, **68**, 1471.
- 18 (a) Z. Qi, Z. H. Zhang, H. L. Jia, Y. J. Qu, G. D. Liu and X. F. Bian, *J. Alloys Compd.*, 2009, **472**, 71–78; (b) Z. H. Zhang, Y. Wang, Z. Qi, W. H. Zhang, J. Y. Qin and J. Frenzel, *J. Phys. Chem. C*, 2009, **113**, 12629–12636.
- 19 R. R. Moskalyk, *Miner. Eng.*, 2004, **17**, 393–402.
- 20 J. Y. Yang, S. G. Lu, S. R. Kan, X. J. Zhang and J. Du, *Chem. Commun.*, 2009, 3273–3275.
- 21 H. Yin, W. Xiao, X. Mao, W. Wei, H. Zhu and D. Wang, *Electrochim. Acta*, 2013, **102**, 369–374.
- 22 (a) W. Xiao, X. Jin and G. Z. Chen, *J. Mater. Chem. A*, 2013, **1**, 10243–10250; (b) W. Xiao and D. H. Wang, *Chem. Soc. Rev.*, 2014, **43**, 3215–3228.
- 23 S. K. Cho, F. R. F. Fan and A. J. Bard, *Angew. Chem., Int. Ed.*, 2012, **51**, 12740–12744.
- 24 J. Zhao, J. Li, P. Ying, W. Zhang, L. Meng and C. Li, *Chem. Commun.*, 2013, **49**, 4477–4479.
- 25 Y. Nishimura, T. Nohira, K. Kobayashi and R. Hagiwara, *J. Electrochem. Soc.*, 2011, **158**, E55–E59.
- 26 A. M. Abdelkader, K. T. Kilby, A. Cox and D. J. Fray, *Chem. Rev.*, 2013, **113**, 2863–2886.
- 27 T. Nohira, K. Yasuda and Y. Ito, *Nat. Mater.*, 2003, **2**, 397–401.
- 28 K. Yasuda, T. Nohira, R. Hagiwara and Y. H. Ogata, *Electrochim. Acta*, 2007, **53**, 106–110.
- 29 E. Juzeliunas, A. Cox and D. J. Fray, *Electrochem. Commun.*, 2010, **12**, 1270–1274.
- 30 M. Beekman, J. A. Kaduk, Q. Huang, W. Wong-Ng, Z. Yang, D. Wang and G. S. Nolas, *Chem. Commun.*, 2007, 837.
- 31 A. Palenzona, P. Manfrinetti and M. L. Fornasini, *J. Alloys Compd.*, 2002, **345**, 144–147.